Optimization of Pulsating Heating in Pool Boiling

J. V. C. Vargas
Assoc. Mem. ASME

A. Bejan
Fellow ASME

Department of Mechanical Engineering
and Materials Science,
Duke University,
Durham, NC 27708-0300

This paper describes an experimental and theoretical study of the periodic on and off heating of water on a horizontal surface. The heat transfer is effected by natural convection and isolated bubbles. The experiments cover the heat flux range 33–154 kW/m^2 and the wall excess temperature range 7–13°C. It is shown experimentally that the cycle-averaged thermal conductance between the surface and the pool can be maximized by properly selecting the time intervals of the on and off heating cycle. The maximum relative augmentation of the thermal conductance is approximately 15 percent. In the second part of the study, an order of magnitude analysis shows that the cycle-averaged thermal conductance can be maximized analytically by considering only the single-phase natural convection effect, and that the optimal time interval when heating is "on" agrees with the experimental results.

Introduction

Several recent studies have shown that pulsating heating can be used to maximize the overall time-averaged thermal conductance between a wall and a flowing fluid (Zumbrunnen, 1992; Kazmierczak and Chinoda, 1992; Lage and Bejan, 1993; Mantle et al., 1994; Antohe and Lage, 1994; Morega et al., 1995; Vargas and Bejan, 1995a, b; Mladin and Zumbrunnen, 1995; Brittingham et al., 1995; Bejan, 1997). The basic idea behind these studies is that the pulsation can be optimally "tuned" to the natural time scale of the flow. There are several ways of inducing pulsations in a convective configuration, for example, in the wall heating pattern, the flow rate, or both.

In the present study we examined the applicability of the pulsating heating process when the heat transfer mechanism is a combination of liquid natural convection and the formation of isolated bubbles. Our objective was to optimize a time-dependent process—a heating strategy—not to design an enhanced heat transfer surface. We used the same surface during the steady state and the many on and off regimes that we studied. We compared these regimes and demonstrated that the on and off regime can be optimized.

A literature survey showed that although there have been many investigations of steady pool boiling, the study of time-dependent pool boiling has attracted very limited attention. For example, Johnson (1971) simulated nuclear reactor excursions by experimenting with water and strips with exponentially increasing heat inputs. His conclusion was that transient nucleate boiling rates for exponential heat inputs are covered reasonably well by steady state nucleate boiling correlation techniques, although large increases in the critical heat flux are possible during highly transient circumstances. Sakurai and Shiotsu (1977a, b) experimented with exponentially heated horizontal wires in a study of reactivity accidents in water cooled nuclear reactors. They found that the transient boiling heat transfer coefficient registered after the commencement of boiling is lower than the steady boiling coefficient at the same heat flux. Bernardin and Mudawar (1994) studied transient boiling during the spray quenching of aluminum parts. Their interest was in achieving faster and more uniform cooling than during bath quenching. They evaluated the temperature-time history of the process and the changes occurring during the quench and concluded that surface roughness enhances the cooling rate significantly. The methods of augmenting nucleate pool boiling heat transfer were reviewed most recently by Thome (1992). Among these, enhanced nucleation, thin film evaporation, and two-phase convection in the reentrant channels (e.g., Nakayama et al., 1980a, b) are recognized as the primary modes for augmenting heat transfer.

A comprehensive review of the literature on quenching phenomena was presented by Nelson and Pasamehmetoglu (1992). This review provides insight into the existing models and covers the fundamental concepts that are relevant to time-dependent boiling. In addition, Pasamehmetoglu and Nelson (1991) documented the effect of site distribution on the nucleate boiling curve. They concluded that as the site distribution becomes less uniform, the average surface temperature and the temperature variations along the boiling surface increase.

In brief, the existing studies of time dependent pool boiling did not consider the optimization of the periodic heating process. The boiling regime considered in this paper is dominated by natural convection with limited bubble generation. The objectives of the present study were to study this phenomenon and to optimize the on and off heating cycle for maximum augmentation effect. In the first part we showed experimentally that the time-averaged heat transfer coefficient for pulsating heating can be greater than for steady heating, and that this augmentation effect can be maximized by properly selecting the pulse period or frequency. In the second part of our study we constructed an order of magnitude analysis, to first explain the existence of an optimal pulse period, and, second, to anticipate analytically the order of magnitude of the optimal pulse period.

Experiments

We began our study with several series of experiments in the natural convection and isolated bubbles regime in a saturated water pool heated from below. The objectives of these experiments were (1) to demonstrate through repeatable measurements the existence of an optimal heat pulse interval for maximum cycle-average thermal conductance, (2) to determine the range of conditions where optimized pulse-heating means "heat transfer augmentation" relative to steady boiling, and (3) to generate a sufficient volume of measurements against which to test the theoretical predictions described in the next section.

Apparatus. The main features of the experimental apparatus are shown in Fig. 1. Water boiled at atmospherical pressure in a well insulated cylindrical vessel made out of aluminum. The wall of the vessel and the heat transfer surface were 1.5

Contributed by the Heat Transfer Division for publication in the JOURNAL OF HEAT TRANSFER. Manuscript received by the Heat Transfer Division August 6, 1996; revision received January 17, 1997; Keywords: Boiling, Natural Convection, Transient & Unsteady Heat Transfer. Associate Technical Editor: R. Nelson.

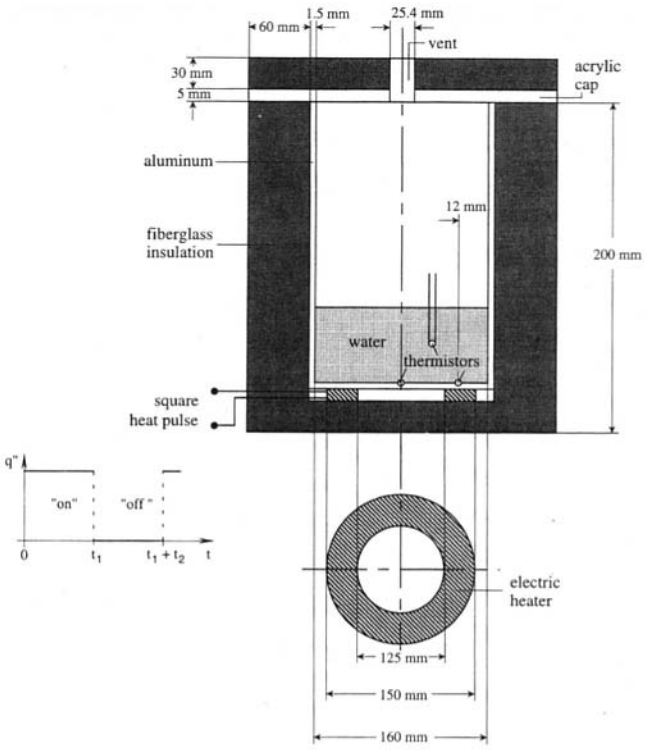

Fig. 1 The main features of the experimental apparatus and the square-wave heat input

mm thick. A flat annular electric heater was attached to the bottom of the aluminum vessel with high conductivity epoxy. The heater has a maximum power of 1200 W at 120 V, and a nominal resistance of 12 Ω. The dimensions of the aluminum vessel and electric heater are indicated directly on Fig. 1. The vessel was covered with an acrylic lid fitted with a boil-off vent. The assembly was wrapped all around with a 6 cm thick layer of fiberglass insulation. It is worth pointing out that the features of the apparatus were selected intentionally to resemble the features of a commercial hot surface for boiling water. We wanted to show that an optimal pulsating boiling regime exists in common (practical) designs, not in idealized laboratory set-ups. In the experiments we compared steady heating with pulsating heating of several frequencies by using the same heat transfer surface. Therefore, given the process optimization objective of our study, the detailed features and defects (e.g., nucleation sites) did not change from one run to the next. Furthermore, as we shall see in the concluding sections of the paper, the effect of bubble formation was dominated by single-phase convection.

Two high precision thermistors (resistance 2250 Ω at 25°C) were embedded to a depth of 1 mm on the water side of the bottom surface of the aluminum vessel. This thermistor type has a standard Bead I with a 2.4 mm diameter. A layer of heat sink silicone was placed between thermistors and aluminum. One thermistor was placed in the center of the bottom surface and the other above the mid-circle of the ring heater. A third thermistor was lowered to various depths in the water pool. Since in the present experiments natural convection was an important mechanism, the presence of the two thermistors was not expected to influence the heat transfer process. This and other features of the simple apparatus used in these experiments are justified because our objective was to optimize a process: we compared many pulsating heating regimes with the steady-state regime by using the same surface.

As shown on the left side of Fig. 1, the pulse is a step function (on and off), with constant heat flux from $t = 0$ to $t = t_1$, and zero heat flux during the next interval of length t_2. We designed and built the adjustable electronics needed to assemble our own square-wave heat pulse generator. The time intervals of the on and off cycle (t_1, t_2) were controlled by a dual timer integrated circuit, which controls a relay that interrupts the power supply. The time ratio t_1/t_2 can be adjusted: in these experiments we used $t_1/t_2 = 0.5$, 1 and 2. All the time interval settings were adjusted using a chronometer with a bias limit of ±0.01 s. The power input to the electric heater was held constant during each t_1-long interval during every run.

The function of the thermistors was to measure the instantaneous temperature of the bottom surface and to identify the maximum temperature of the bottom surface (T_{max}) during the on and off cycle. The maximum difference between the readings provided by the bottom thermistor placed above the heater and the thermistor placed in the center of the bottom wall was 0.6°C. This suggests that the heat transfer surface corresponded to a sufficiently uniform site distribution: recall that a nonuniform site distribution promotes a large span between the minimum and maximum surface temperatures, cf. Pasamehmetoglu and Nelson (1991). Since the average temperature is the quantity used in plotting the steady-state boiling curve, the results obtained in this study can be compared with previously published results.

The third thermistor monitored the water pool temperature during each run: this temperature was invariably the saturation temperature T_{sat} = 100°C, with deviations less than ±0.1°C. According to the manufacturer (YSI, 1993), the time needed by the thermistor to indicate a newly impressed temperature is less than 1 s when the temperature difference is 200°C. Since in the present experiments the maximum temperature difference was 13°C, we are confident that our temperature measurements were accurate even sooner, for example, after 0.5 s.

The thermistor readings were taken with an ohmmeter capable of measuring resistances as small as 10^{-3} Ω in the temperature range near the saturation temperature, and as small as 10^{-4} Ω in the range near the nominal resistance of the heater. In this way we were able to measure the maximum temperature difference that occurs during steady-periodic heat transfer conditions, $\Delta T_{max} = T_{max} - T_{sat}$. By convention, the steady-periodic

Nomenclature

A = heat transfer area
B = bias limit
g = gravitational acceleration
k = thermal conductivity of liquid water
P = precision limit
q'' = heat flux during t_1 interval
$\bar{q}''$ = cycle-averaged heat flux
R = heater resistance
t = time
t_{th} = time scale of thermal formation
t_1 = time interval when heater is on
t_2 = time interval when heater is off
T = temperature
ΔT = wall excess temperature, $T - T_{sat}$
U = uncertainty limit
V = voltage
α = thermal diffusivity of liquid water
β = coefficient of volumetric thermal expansion
δ = thermal diffusion thickness
ν = kinematic viscosity of liquid water

Subscripts

max = maximum
opt = optimal
sat = saturation
th = thermals

Table 1 Measured times and maximum temperature differences, and the uncertainties in the pulsating heat experiments, each pair of values represents ΔT_{max} (°C)/$U_{\Delta T_{max}}$ (°C)

t_1 (s)	q'' (kW/m²) = 100			154.3		
	t_1/t_2 = 0.5	1	2	0.5	1	2
0.5		7.922/0.078				
0.7	6.763/0.100				9.336/0.090	
0.8		7.828/0.102		8.460/0.120		
1.0						10.251/0.086
1.5		7.642/0.111				
1.6			8.390/0.150			
1.8					9.108/0.172	
2.0	6.509/0.104			8.150/0.086		
2.3						10.062/0.104
2.6			8.292/0.144			
3.0		7.534/0.072			8.909/0.136	
3.4	6.658/0.144		8.119/0.190			
4.0				8.744/0.112		
4.2					8.862/0.160	
4.4						9.964/0.106
5.0		7.470/0.065	7.820/0.150			10.02/0.160
5.4					9.160/0.170	
6.0		7.520/0.082				
6.5	7.558/0.152					
7.0		7.610/0.093		9.336/0.126		10.17/0.106
7.2			7.876/0.100			
7.4					10.001/0.108	
8.0		7.750/0.081				
8.7	7.899/0.100					
10.0		8.124/0.076				
11.0						10.62/0.174
13.0					10.777/0.150	
14.0		8.520/0.068	9.183/0.200			
15.0				10.921/0.198		11.032/0.138
20.0			9.650/02.00			
23.0	8.882/0.144	9.120/0.128				
30.0					11.537/0.224	
34.0				11.75/0.188		
37.0						12.107/0.172
60.0	9.479/0.246	9.716/0.299	10.08/0.158	11.86/0.268	11.927/0.252	12.323/0.208

regime was reached when the wall temperature history during one on and off cycle matched the history of the next cycle within a specified (small) temperature band, which in this study was set at ±0.5°C. The ±0.5°C deviation occurred either in the very beginning of the cycle or in the final part of the cycle, with little influence on T_{max} and the cycle-averaged temperature. The largest observed deviation of T_{max} (plateau temperature) was ±0.1°C in the steady-periodic regime. The possible influence of the overall water circulation (tank geometry) was investigated by varying the pool depth. Since no significant change in T_{max} was detected, all the runs were conducted by using the same pool depth.

The heat flux generated during the t_1 ("on") interval q'' was adjusted through a variable resistor the voltage (V) of which was set at 80 and 100 V. The corresponding cycle-averaged heat flux was calculated using

$$\bar{q}'' = \frac{V^2}{RA(1 + t_2/t_1)} = \frac{q''}{1 + t_2/t_1} \tag{1}$$

where R and A are the resistance and the contact surface of the heater, respectively. It is worth noting that the choice of measuring ΔT_{max} (as opposed to the average temperature difference $\overline{\Delta T}$) is conservative since later we are reporting and comparing the values of the heat transfer coefficient $\bar{q}''/\Delta T_{max}$, which is smaller than $\bar{q}''/\overline{\Delta T}$.

Procedure. We performed our own thermistor calibration to determine the bias limits. The thermistor was immersed in a constant temperature bath maintained by a bath circulator, and a total of 64 temperature measurements were made at 80, 90, . . . , 120°C. The bias limit was set at ±0.001°C for all thermistors (Howle et al., 1992; Dally et al., 1993). The precision limits for the heat flux calculated with Eq. (1) were determined using the propagation line of Kline and McClintock (Editorial, 1993):

$$\frac{P_{\bar{q}''}}{\bar{q}''} = 2\frac{P_V}{V} \tag{2}$$

$$\frac{B_{\bar{q}''}}{\bar{q}''} = \frac{[1 + (t_2/t_1)^2]^{1/2}}{1 + t_2/t_1} \cdot \frac{B_{t_1}}{t_1}. \tag{3}$$

The laboratory is a temperature controlled environment without windows, therefore, the variations in room pressure, temperature, and humidity were negligible. In the calculation of the precision limit for the measured $\bar{q}''$, the contributions made by the precision limits of t_1, t_2, R, and A were found to be negligible relative to the precision limit of V. The time measurement contributions were negligible because once the electronic timer was adjusted, the time intervals were reproduced identically in all the runs. In the calculation of the bias limits for $\bar{q}''$, the time bias limit was the most important contribution because the voltage and resistance bias limit provided by the multimeter, $\pm 10^{-6}$ V and $\pm 10^{-4}$ Ω, respectively, were very small in comparison with the time bias limit of the chronometer used in the timer adjustment.

The precision limit for the measured t_1 was negligible relative to the bias limit in the calculation of the uncertainty because an electronic time control method was used. The precision limit for the temperature measurements was calculated as twice the standard deviation of each set (ten values per point) of observations for ΔT_{max}. The uncertainty limits for ΔT_{max}, $\bar{q}''$, and t_1

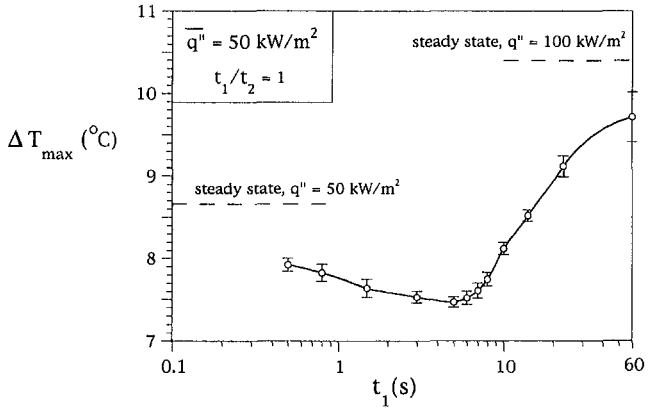

Fig. 2 The effect of the heat pulse interval t_1 on the maximum temperature difference between the wall and the water pool

were calculated using the standard formulas (Editorial, 1993), and the results are summarized in Table 1. In addition, U_{t_1} was equal to 0.01 s in all measurements, and the largest computed $U_{\bar{q}''}/\bar{q}''$ was 0.022.

Results. Figure 2 shows the main features of the measurements collected during one run. The heat flux during the "on" interval was fixed at $q'' = 100$ kW/m^2, and so was the on/off time ratio, $t_1/t_2 = 1$. The corresponding (fixed) cycle-averaged heat flux was $\bar{q}'' = 50$ kW/m^2. Steady-periodic regimes were created for 12 different t_1 values that cover the range 0.5 s–60 s. The bias limit of the chronometer used in the calibration of the electronic timer was 0.01 s, therefore, we found it appropriate to use t_1 intervals greater than 0.5 s to guarantee the accuracy of the measured time intervals. The measured ΔT_{max} values and the calculated precision limits show that ΔT_{max} is minimum when t_1 is approximately 5 s. This means that the thermal conductance $\bar{q}''/\Delta T_{max}$ between the wall and the water pool is maximum at a certain measurable pulse period or frequency.

Figure 2 also shows the ΔT_{max} measurements made in the two t_1 extremes. The $t_1 \to \infty$ limit means that the heater is left "on" forever (at $q'' = 100$ kW/m^2), which is why we wrote "steady state" next to the dashed line, indicating the measured ΔT value. In reality, when t_1 is large but finite, the wall temperature exhibits wide excursions between the $t_1 \to \infty$ asymptote (ΔT_{max}) shown in the figure and the lowest temperature in the system (T_{sat}). The opposite extreme, $t_1 \to 0$, corresponds to steady heating at a q'' value that is equal to the cycle-averaged value, namely, 50 kW/m^2. The measured steady ΔT value is also indicated with a dashed horizontal line: it is with respect to this line that we evaluate the thermal contact augmentation effect achieved by fine-tuning t_1. The minimum ΔT_{max} value registered at $t_1 \cong 5$ s was 14 percent smaller than the steady ΔT measured in the $t_1 \to 0$ limit.

We found that the features of the run presented in Fig. 2 were reproduced by the data collected in all the runs (total runs = 6). Three additional examples are illustrated in Figs. 3(a, b) and 4 where we note that the precision limits on ΔT_{max} are nearly the same as in Fig. 2. Figures 3(a) and 3(b), in association with Fig. 2, show the effect of varying the on/off ratio t_1/t_2 while holding the "on" heat flux q'' fixed. Three changes occur as t_1/t_2 increases: $\bar{q}''$ increases, the steady ΔT value measured in the $t_1 \to 0$ limit increases, and the minimum of the ΔT_{max} versus t_1 curve shifts toward larger optimal t_1 values.

Figure 4 should be compared with Fig. 2 to see what changes occur when the run is repeated at a higher heat flux during the "on" interval. All the ΔT_{max} measurements rise, however, the shape of the ΔT_{max} versus t_1 curve does not change. Even the optimal t_1 interval for minimum ΔT_{max} appears to be insensitive to the increase in q'' from Fig. 2 to Fig. 4.

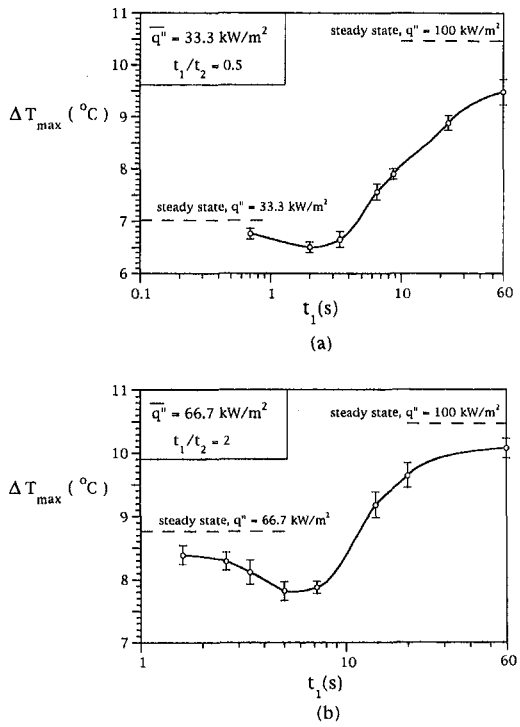

Fig. 3 The effect of changing the time ratio t_1/t_2 relative to the run exhibited in Fig. 2

Figures 5(a) and 5(b), in combination with Fig. 4, show the effect of changing the time ratio t_1/t_2 when the heat flux is high: $q'' = 154.3$ kW/m^2. Once again, the optimal t_1 interval increases as t_1/t_2 increases: this observation reinforces the trend revealed by the runs conducted at the lower heat flux (Figs. 2, 3(a, b)).

To summarize, Figs. 2–5 demonstrate conclusively that an optimal on and off period exists such that the thermal conductance $\bar{q}''/\Delta T_{max}$ is maximized. Figures 6 and 7 summarize the maximum thermal conductance and optimal pulse interval results obtained in the experimental phase of our study. Although the increase in $\bar{q}''/\Delta T_{max}$ registered when t_1 is optimal is generally of the order of 15 percent, the results of Fig. 6 indicate that maximum augmentation occurs when t_1/t_2 is close to 1. Figure 6 also suggests that the augmentation effect becomes stronger as the heat flux decreases: to this effect we return in the next section. Figure 7 summarizes the $t_{1,opt}$ trends noted

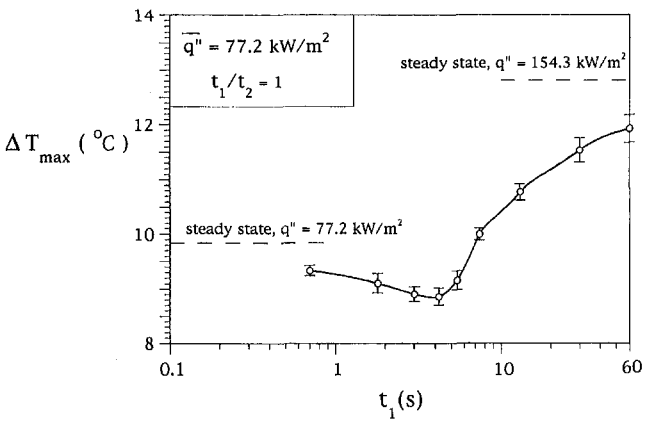

Fig. 4 The effect of increasing the heat flux q'' relative to the run exhibited in Fig. 2

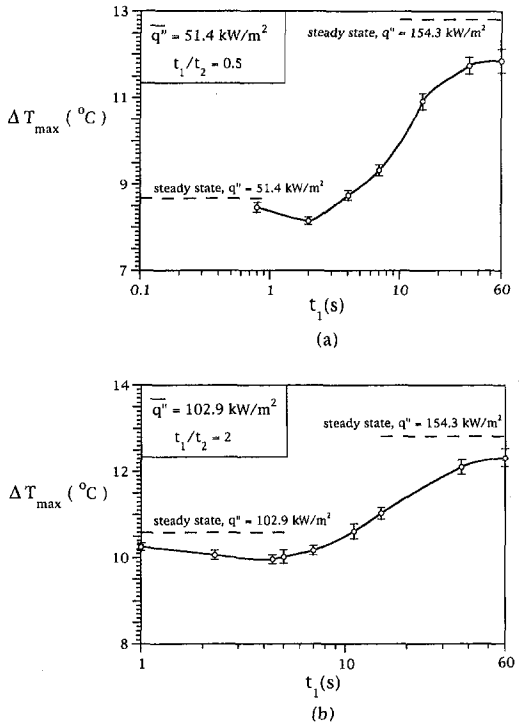

Fig. 5 The effect of changing the time ratio t_1/t_2 relative to the run exhibited in Fig. 4

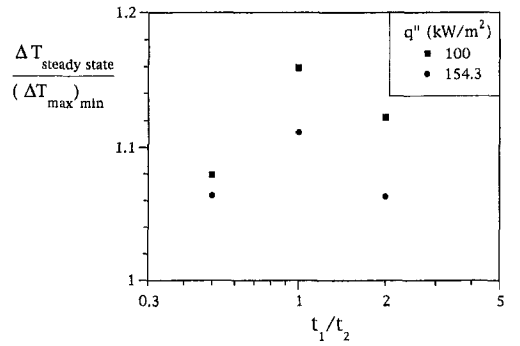

Fig. 6 Summary of the maximum heat transfer augmentation results determined experimentally

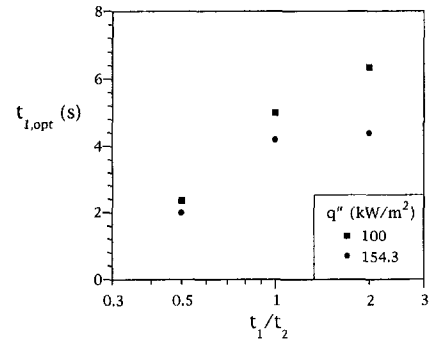

Fig. 7 Summary of the optimal heat-interval results determined experimentally

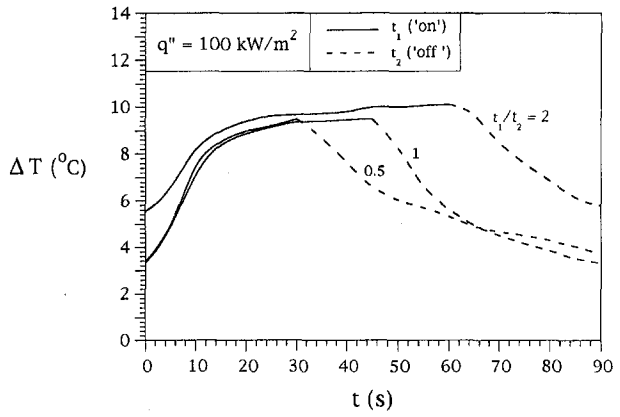

Fig. 8 The wall temperature history during a complete on and off cycle

earlier, namely, that $t_{1,opt}$ increases as t_1/t_2 increases, and that $t_{1,opt}$ is relatively insensitive to increasing the heat flux. The augmentation phenomenon is related to the effect reported by Zumbrunnen and Balasubramanian (1995) in which the air bubbles injected into an impinging liquid jet triggered the renewal of the boundary layer. The augmentation effect maximized in Figs. 2–7 was measured relative to the steady-state regime associated with a heat flux equal to the cycle-averaged heat flux (see the $t_1 \rightarrow 0$ asymptotes in Figs. 2–5).

As an introduction to the theoretical argument constructed in the next section, we end this experimental part with a view of the temperature history of bottom wall surface during a complete on and off cycle after a sufficiently long experiment in which the steady-periodic regime was well established. The three ΔT versus t traces shown in Fig. 8 were recorded with the thermistor placed right above the heater (Fig. 1), and correspond to the $q'' = 100$ kW/m^2 runs seen earlier in Figs. 2, 3(a), and 3(b). One point is exhibited from each one of these figures, as seen in the following table:

	$t_1/t_2 = 0.5$ (Fig. 3a)	$t_1/t_2 = 1$ (Fig. 2)	$t_1/t_2 = 2$ (Fig. 3b)
t_1	30 s	45 s	60 s
$t_1 + t_2$	90 s	90 s	90 s

For example, in Fig. 8 the $t_1/t_2 = 2$ curve shows that the wall temperature increases, reaching a plateau during the "on" time interval. The maximum ΔT recorded during this interval is the ΔT_{max} value presented in Figs. 2–5. The wall temperature decays partially during the "off" time interval. The key message of the periodic variation of ΔT versus t is that the wall thermal inertia plays a role, which, as we show next, is important because it smoothes (tends to hide) the effect of t_1 on the minimization of ΔT_{max}. The wall inertia is also important because it is a permanent feature in the construction of commercial hot surfaces for boiling water.

Theoretical Considerations

The existence of an optimal "on" interval can be anticipated based on a scale analysis of the time-dependent development of natural convection in the liquid phase. Assume that the heating (q'') is turned on at $t = 0$ and that the liquid is motionless. The thickness of the water layer heated by the bottom surface increases in time because of thermal diffusion,

$$\delta \sim (\alpha t)^{1/2}. \tag{4}$$

The temperature difference between the wall and the bulk liquid (ΔT) must also increase as $t^{1/2}$ because q'' is constant:

$$\Delta T \sim \frac{q''}{k}\,\delta. \tag{5}$$

The heated layer (δ) becomes unstable and gives birth to thermals at a time (t_{th}) when the Rayleigh number based on height [$\delta_{th} \sim (\alpha t_{th})^{1/2}$] and vertical temperature difference ($\Delta T_{th} \sim q''\delta_{th}/k$) become comparable with the order of magnitude associated with the onset of Benard convection (Bejan, 1993; p. 372):

$$\frac{g\beta}{\alpha\nu}\,\delta_{th}^3 \Delta T_{th} \sim 2000. \tag{6}$$

Combining Eqs. (4)–(6) we find that the time scale for the formation of thermals is

$$t_{th} \sim \left(2000\,\frac{k\nu}{q''\alpha g\beta}\right)^{1/2}. \tag{7}$$

By substituting $q'' = 10^5$ W/m^2 and the properties of saturated water at 100°C into Eq. (7) we find $t_{th} \sim 2$ s, which in the language of scale analysis means "seconds." This time scale agrees with the time scale of the present experiments and is orders of magnitude greater than the time scale of bubble formation.

The heating process continues until $t = t_1$. We distinguish two scenarios depending on whether t_1 is smaller or greater than t_{th}.

$t_1 < t_{th}$. When thermals do not form while the heating is on, the excess temperature ΔT reaches its highest value at the end of the heating interval:

$$\Delta T_{max} \sim \frac{q''}{k}\,(\alpha t_1)^{1/2}. \tag{8}$$

Equations (1) and (8) show that the overall thermal conductance varies as $t_1^{1/2}/(t_1 + t_2)$:

$$\frac{\overline{q''}}{\Delta T_{max}} \sim \frac{k}{\alpha^{1/2}} \cdot \frac{t_1^{1/2}}{t_1 + t_2}. \tag{9}$$

This quantity has a maximum with respect to t_1 that occurs when

$$t_{1,opt} = t_2. \tag{10}$$

This behavior and the order-of-magnitude conclusion, $t_{1,opt} \sim t_2$, are supported by the minima of the ΔT_{max} curves determined experimentally (Figs. 2–5).

It is worth noting that we reach the same conclusion if, instead of ΔT_{max}, we use the time averaged temperature difference $\overline{\Delta T}$ in the heat transfer coefficient defined in Eq. (9). Specifically, according to Eqs. (4) and (5) the temperature difference averaged over the interval t_1 is simply $\overline{\Delta T} = (\frac{2}{3})\Delta T_{max}$, because ΔT increases as $t^{1/2}$. In other words, the definition of the heat transfer coefficient does not change the analytical form of Eq. (9), which is dictated by the function $t_1^{1/2}/(t_1 + t_2)$.

$t_1 > t_{th}$. When the heating interval extends beyond the departure time of thermals, the time growth of δ and ΔT is terminated at $t \sim t_{th}$. This event is characterized by the maximum temperature difference

$$\Delta T_{max} \sim \frac{q''}{k}\,(\alpha t_{th})^{1/2} \tag{11}$$

which is fixed by t_{th}, i.e., constant, not a function of t_1. If t_1 is considerably greater than t_{th}, then a number ($\sim t_1/t_{th}$) of thermals rise successively from the same region of the wall, and the maximum temperature difference continues to be represented by the ceiling given in Eq. (11). In combination with Eq. (1), this conclusion means that the overall thermal conductance effect due to liquid natural convection,

$$\frac{\overline{q''}}{\Delta T_{max}} \sim \frac{k}{(\alpha t_{th})^{1/2}}\,\frac{t_1}{t_1 + t_2}, \tag{12}$$

does not exhibit a maximum with respect to t_1, in fact it levels off at constant of order $k/(\alpha t_{th})^{1/2}$.

In summary, to search for a conductance maximum we must look in the opposite direction (decreasing t_1) and, according to the first scenario ($t_1 < t_{th}$), the maximum manifests itself first when $t_1 \sim t_{th}$. Combining this with Eq. (10) we conclude that the conductance maximum occurs when the heat pulse matches the time scale of single-phase natural convection:

$$t_{1,opt} \sim t_2 \sim t_{th}. \tag{13}$$

This conclusion is in accord with all our experiments. We saw that the optimal t_1 and t_2 intervals measure several seconds as the t_{th} scale for saturated liquid water.

A more direct alternative to Eq. (13) is to recognize first the natural time scale of single-phase natural convection (thermals), Eq. (7), and to argue that the maximum thermal conductance occurs when the heat pulses are in step with t_{th}. This "resonance" argument is supported by several earlier studies which were reviewed in the introduction. In the present case (significant single-phase natural convection with isolated bubbles) resonance means that the on and off heating administered by the wall has the ability to "organize", in time and space, the formation and departure of thermals. This interaction is similar to the organization displayed by turbulent jets exposed to a lateral loud speaker (e.g., buoyant plume, Kimura and Bejan, 1983).

Next to the time scale of a few seconds, another feature that supports the view that the conductance maximum is governed by the time scale of single-phase natural convection is the fact that the augmentation effect (Figs. 2–5) decreases as q'' and ΔT increase. The opposite direction—a sharper maximum at smaller q'' and ΔT—means that the augmentation effect is a natural convection feature. Further support is provided by the recent study of Ammerman and You (1996): their Fig. 9 shows that at a heat flux of 100 kW/m^2, the heat transfer by boiling (latent heat, bubble generation) is roughly 50 percent, and it increases to about 75 percent when the heat flux is 150 kW/m^2. This means that in the same range, the importance of natural convection diminishes, which agrees with the phenomenological explanation provided in this section.

Conclusion

In this study we showed experimentally that the on and off heating cycle of a surface with pool boiling can be optimized for maximum cycle-averaged thermal conductance. There is an optimal period or frequency of pulse heating (Figs. 2–7), and among these optimal results there is an optimal on/off time ratio, $t_{1,opt} \sim t_2$ (Fig. 6).

The present water experiments covered only the ΔT range associated with the combined effects of liquid natural convection and isolated bubbles. It is quite probable that the augmentation optimization principle demonstrated experimentally can be exploited at other ΔT's along the boiling curve, especially in the direction $\Delta T \to 0$, as well as in single-phase natural convection without boiling.

The maximum relative augmentation effect of approximately 15 percent (Fig. 6) is a realistic indicator of what can be accomplished in practice by fine-tuning the on and off heating cycle. It is realistic because the experimental apparatus had the features of a commercial water heater, namely, wall thermal inertia, and fin conduction along the wall, from heated spots to unheated spots. Such features tend to smooth the $\Delta T(t)$ variation during the on and off cycle and to obscure the optimization with respect

to t_1. It is quite probable that a maximum relative augmentation greater than 15 percent could be achieved with special laboratory apparatuses in which the wall inertia and fin effects are absent. Such a possibility deserves future study, especially now that the on and off optimization principle was demonstrated under conservative conditions.

Regarding the size of the increase in heat transfer coefficient (large or small?) the appropriate design question is quite different: "What is the easiest (cheapest, most robust) way to achieve this increase?" To pulsate the electrical current through the heater is attractive, in comparison with other (e.g., mechanical, invasive) methods. This is why pulsating heat transfer and unsteady heating, in general, are attracting interest across the wide spectrum of heat transfer engineering (Bejan, 1996).

Acknowledgment

This research was supported by a grant from the National Science Foundation.

References

Ammerman, C. N., and You, S. M., 1996, "Determination of the Boiling Enhancement Mechanism Caused by Surfactant Addition to Water," ASME JOURNAL OF HEAT TRANSFER, Vol. 118, pp. 429–435.

Antohe, B. V., and Lage, J. L., 1994, "A Dynamic Thermal Insulator: Inducing Resonance Within a Fluid Saturated Porous Medium Enclosure Heated Periodically from the Side," *International Journal of Heat Mass Transfer,* Vol. 37, pp. 771–782.

Bejan, A., 1993, *Heat Transfer,* John Wiley and Sons, New York, p. 187.

Bejan, A., 1996, "Fundamental Optima in Thermal Science: Time-Dependent (On and Off) Processes," in Manglik, R. M. and Kraus, A. D., eds., *Process, Enhanced, and Multiphase Heat Transfer: A Festschrift for A. E. Bergles,* Begell House, New York, pp. 51–57.

Bejan, A., 1997, "Theory of Organization in Nature: Pulsating Physiological Processes," *International Journal of Heat and Mass Transfer,* Vol. 40, pp. 2097–2104.

Bernardin, J. D., and Mudawar, I., 1994, "An Experimental Investigation into the Relationship Between Temperature-Time History and Surface Roughness in the Spray Quenching of Aluminum Parts," ASME HTD-Vol. 289, pp. 63–71.

Brittingham, R. A., Mladin, E. C., and Zumbrunnen, D. A., 1995, "Heat Transfer Transients in Stagnation Flows Due to Changes in Flow Velocity," *Journal of Thermophysics and Heat Transfer,* Vol. 10, pp. 186–189.

Dally, J. W., Riley, W. F., and McConnell, K. G., 1993, *Instrumentation for Engineering Measurements,* John Wiley and Sons, New York, p. 425.

Editorial, 1993, ASME JOURNAL OF HEAT TRANSFER, Vol. 114, pp. 5–6.

Howle, L., Georgiadis, J., and Behringer, R., 1992, "Shadowgraphic Visualization of Natural Convection in Rectangular-Grid Porous Layers," ASME HTD-Vol. 206-1, pp. 17–24.

Johnson, H. A., 1971, "Transient Boiling Heat Transfer to Water," *International Journal of Heat and Mass Transfer,* Vol. 14, pp. 67–82.

Kazmierczak, M., and Chinoda, Z., 1992, "Buoyancy-Driven Flow in an Enclosure with Time Periodic Boundary Conditions," *International Journal of Heat Mass Transfer,* Vol. 35, pp. 1507–1518.

Kimura, S., and Bejan, A., 1983, "Mechanism for Transition to Turbulence in Buoyant Plume Flow," *Int. J. Heat Mass Transfer,* Vol. 26, pp. 1515–1532.

Lage, J. L., and Bejan, A., 1993, "The Resonance of Natural Convection in an Enclosure Heated Periodically from the Side," *International Journal of Heat Mass Transfer,* Vol. 36, pp. 2027–2038.

Mantle, J., Kazmierczak, M., and Hiawy, B., 1994, "The Effect of Temperature Modulation on Natural Convection in a Horizontal Layer Heated from Below: High-Rayleigh-Number Experiments," ASME JOURNAL OF HEAT TRANSFER, Vol. 116, pp. 614–620.

Mladin, E. C., and Zumbrunnen, D. A., 1995, "Dependence of Heat Transfer to a Pulsating Stagnation Flow on Pulse Characteristics," *Journal of Thermophysics and Heat Transfer,* Vol. 9, pp. 181–190.

Morega, A. M., Vargas, J. V. C., and Bejan, A., 1995, "Optimization of Pulsating Heaters in Forced Convection," *International Journal of Heat and Mass Transfer,* Vol. 38, pp. 2925–2934.

Nakayama, W., Daikoku, T., Kawahara, H., and Nakajima, T., 1980a, "Dynamic Model of Enhanced Boiling Heat Transfer on Porous Surfaces. Part I: Experimental Investigation," ASME JOURNAL OF HEAT TRANSFER, Vol. 102, pp. 445–450.

Nakayama, W., Daikoku, T., Kawahara, H., and Nakajima, T., 1980b, "Dynamic Model of Enhanced Boiling Heat Transfer on Porous Surfaces. Part II: Analytical Modeling," ASME JOURNAL OF HEAT TRANSFER, Vol. 102, pp. 451–456.

Nelson, R. A., and Pasamehmetoglu, K. O., 1992, "Quenching Phenomena," *Post-Dryout Heat Transfer,* G. F. Hewitt, J. M. Delhaye, and N. Zuber, eds., CRC Press, Boca Raton, FL, pp. 39–184.

Pasamehmetoglu, K. O., and Nelson, R. A., 1991, "Cavity-to-Cavity Interaction in Nucleate Boiling: The Effect of Heat Conduction within the Heater," *AIChE Symposium Series, Heat Transfer,* No. 283, Vol. 87, pp. 342–351.

Sakurai, A., and Shiotsu, M., 1977a, "Transient Pool Boiling Heat Transfer. Part 1: Incipient Boiling Superheat," ASME JOURNAL OF HEAT TRANSFER, Vol. 99, pp. 547–553.

Sakurai, A., and Shiotsu, M., 1977b, "Transient Pool Boiling Heat Transfer. Part 2: Boiling Heat Transfer and Burnout," ASME JOURNAL OF HEAT TRANSFER, Vol. 99, pp. 554–560.

Thome, J. R., 1992, "Mechanisms of Enhanced Nucleate Pool Boiling," Engineering Foundation Conference on Pool and External Flow Boiling, ASME, NY, pp. 337–343.

Vachon, R. I., Nix, G. H., and Tanger, G. E., 1968, "Evaluation of Constants for the Rohsenow Pool-Boiling Correlation," ASME JOURNAL OF HEAT TRANSFER, Vol. 90, pp. 239–247.

Vargas, J. V. C., and Bejan, A., 1995a, "Optimization Principle for Natural Convection Pulsating Heating," ASME JOURNAL OF HEAT TRANSFER, Vol. 117, pp. 942–947.

Vargas, J. V. C., and Bejan, A., 1995b, "Fundamentals of Ice Making by Convection Cooling Followed by Contact Melting," *International Journal of Heat and Mass Transfer,* Vol. 38, pp. 2833–2841.

YSI Temperature Sensors & Probes Manual, 1993, YSI Inc., Yellow Springs, OH.

Zumbrunnen, D. A., 1992, "Transient Convective Heat Transfer in Planar Stagnation Flows with Time-Varying Surface Heat Flux and Temperature," ASME JOURNAL OF HEAT TRANSFER, Vol. 114, pp. 85–92.

Zumbrunnen, D. A., and Balasubramanian, M., 1995, "Convective Heat Transfer Enhancement Due to Gas Injection Into an Impinging Liquid Jet," ASME JOURNAL OF HEAT TRANSFER, Vol. 117, pp. 1011–1017.